

## Effect of Copper(II) Ions on Corrosion Resistance of Al-Zn Coated 5052 Aluminum Alloy in Seawater

Guofeng Lv<sup>1,\*</sup>, Yanming Xia<sup>2</sup>, Xiong Chen<sup>1</sup>, Zhao Liu<sup>1</sup>, Fang Zhuang<sup>1</sup>, Zhiming Gao<sup>2,\*</sup>

<sup>1</sup> Petrochina Jiangsu LNG Company Limited, Nantong, 226001, China

<sup>2</sup> Engineering Research Center of Composite and Functional Materials, School of Materials Science and Engineering, Tianjin University, Tianjin, 300072, China

\*E-mail: [lvgf169@petrochina.com.cn](mailto:lvgf169@petrochina.com.cn), [gaozhiming@tju.edu.cn](mailto:gaozhiming@tju.edu.cn)

Received: 5 May 2021 / Accepted: 27 July 2021 / Published: 10 September 2021

---

The corrosion resistance of the composite anti-corrosion coating formed by an aluminum-zinc coating and epoxy sealer on the surface of an open rack vaporizer (ORV) in seawater was investigated at different copper ion ( $\text{Cu}^{2+}$ ) concentrations. The surface microstructure of the coating was characterized by ultra-field 3D observation, SEM and energy spectrum analysis (EDS). The sealer was found to be effective in shielding the coating surface and significantly reduced the corrosion rate of the coating. A dissolution process of the passive film on the coating surface is evident from the potentiodynamic polarization curves and surface morphology. Local corrosion occurs on the coating surface, and the number and area of surface corrosion pits increase with the concentration of copper in solution, indicating a decrease of the corrosion resistance of the coating. Weight loss of the samples increases from 4.5 mg to 5.4 mg after a 32 days immersion, and the damage of copper ions on the coating originates from weak positions of the surface. The electrochemical corrosion behavior of the coating was investigated by dynamic potential polarization and electrochemical impedance spectroscopy (EIS), with a positive effect found after a short immersion period in a solution with copper ion concentration lower than 5  $\mu\text{g/L}$ , with this effect not evident at higher copper concentrations.

---

**Keywords:** Copper ions, composite coating, corrosion morphology, potentiodynamic polarization;, electrochemical impedance spectroscopy

### 1. INTRODUCTION

Aluminum alloys are widely used in various industrial applications due to their good strength-to-weight ratio and corrosion resistance properties[1-3]. In the energy industry, aluminum alloys have replaced traditional materials such as copper alloys and stainless steels and are widely integrated into heat exchange systems[4]. It is recognized that the good corrosion resistance of aluminum and its alloys comes from a layer of passive film generated on the surface, which will be damaged by local corrosion[5-

8] in acidic, alkaline and humid aggressive environments and media containing chlorides, causing corrosion failure of aluminum components and even serious engineering accidents and economic losses. The open rack vaporizer (ORV) is a heat exchanger for gasification of liquefied natural gas (LNG) using seawater as the heat medium, with low operating costs and simple operation, and is one of the key equipment for LNG receiving stations. The heat exchanger tube of ORV is made of aluminum alloy, and the marine environment where it is applied itself is a weak acidic environment with high humidity and a large amount of chlorides[9, 10], which can easily damage the aluminum equipment. Also seawater contains a variety of heavy metal ion contaminants including  $\text{Cu}^{2+}$ , in addition to the fact that aluminum equipment is often connected to copper components during application[11-13], and the metal ions generated by dissolution can diffuse into the medium and have a complex effect on the corrosion process of aluminum equipment[14, 15]. Khedr[16] et al. found that in neutral and acidic  $\text{Cl}^-$ -containing solutions, when the addition of some heavy metal ions, including  $\text{Cu}^{2+}$ , is added at low concentrations, the electrons required for the cathodic reaction on the surface of aluminum alloys are consumed by the replacement deposition reaction of the cation corresponding to the metal causing corrosion to slow down; while at higher concentrations, a large number of metals are deposited and form an electric couple with aluminum, and the galvanic corrosion effect is intensified, thus greatly accelerating the corrosion rate of aluminum. Joseph[17] et al. conducted wet/dry cycle corrosion tests in natural seawater revealed that in copper/aluminium samples, aluminium and copper acted as anode and cathode, respectively, causing significant corrosion of aluminium, which was significantly accelerated as evidenced by the aluminium oxide clusters on the surface of the copper specimens and the very low levels of  $\text{Cu}^{2+}$  in the solution. Gao[18] investigated the effect of copper ions on the corrosion behavior of 5A02 aluminum alloy in aqueous ethylene glycol solution and concluded that the corrosion potential was positively shifted and the corrosion current increased due to the deposition of copper. The main type of corrosion under this condition was pitting, and the pitting density was positively correlated with copper ion concentration. And at the defects around the second phase, copper ions were preferentially deposited to form Al-Cu micro-couples, which accelerated the corrosion rate of aluminum.

Although work on the effect of copper ions on the corrosion process of aluminum and its alloys in different media has been carried out, the materials used in previous studies were mostly pure aluminum or polished aluminum alloy specimens. In practical applications, protective coatings are usually applied to various metal surfaces in order to protect or mitigate the corrosion process[19-23]. Zeng[24] et al. prepared coatings on aluminum alloy substrates by plasma electrolytic oxidation (PEO) and further prepared silicone sealants on PEO coatings by sol-gel method to form composite coatings with them, which effectively sealed microdefects and improved the corrosion resistance of the coatings in different corrosive solutions, thus verifying the effectiveness of the sealants in different corrosive solutions and expanding their application scope. Although the coating of sealants on the surface of aluminum alloys can effectively improve the corrosion resistance of components[25-27], there are fewer studies on the effect of heavy metal  $\text{Cu}^{2+}$  ions in seawater on components with sealants, and the mechanism of the effect of  $\text{Cu}^{2+}$  on their corrosion process is unclear, despite the excellent performance of sealants in practical applications.

In this work, AA5052[28-30], a typical material used in the energy industry, was used, and a composite layer of aluminum-zinc alloy coating (Al98%-Zn2%) and epoxy resin-based sealer was

applied to its surface by thermal spraying to prevent corrosion of the substrate, where the sealer acting as a sealer and isolator. The aluminum-zinc alloy coating has a lower potential than the ORV body aluminum alloy and acts as a sacrificial anode to prevent corrosion of the base material. The corrosion resistance of the composite coating in 3.5% wt. NaCl solution with different  $\text{Cu}^{2+}$  content was measured by building an electrochemical experiment platform of immersion to investigate the damage mechanism of  $\text{Cu}^{2+}$  on the coating in seawater, which is of guiding significance to grasp the influence of  $\text{Cu}^{2+}$  on the coating and optimize the selection of coating and sealer materials.

## 2. EXPERIMENTAL

### 2.1 Material and solution preparation

In this experiment, in order to investigate the corrosion effect of seawater  $\text{Cu}^{2+}$  concentration on the corrosion resistance of typical materials used in ORV, 5052 aluminum alloy substrate was flame sprayed with Al98%-Zn2% coating, coated with epoxy resin sealer and processed into a 15mm×15mm test block. The wire was welded to the surface of the specimen, and the specimen was cold sealed with epoxy resin on the surface other than the working surface. The treated specimen was ultrasonically degreased with alcohol and washed with distilled water and then blown dry and set aside. In the full immersion experiment, different masses of copper chloride were added to the 3.5% wt. NaCl solution to prepare the solution for the experiment, and eventually the 3.5% wt. NaCl solutions with copper ion content of 5, 50 and 110 ug/L were obtained. And 3.5% wt. NaCl solution was used as the control group.

### 2.2 Experiment method

Full immersion corrosion method was used to investigate the influence of copper ion concentration on the corrosion resistance of coatings. The open circuit potential of the specimens was measured using PARSTAT2273 electrochemical workstation after 8, 16 and 32 days of immersion in 3.5% wt. NaCl solution with copper ion content of 5, 50 and 110 ug/L, and the electrochemical impedance spectrum (EIS) and potentiodynamic polarization curves were measured after stabilization with a conventional three-electrode system, where platinum sheet was the auxiliary electrode, saturated glycury electrode was used as the reference electrode, and the specimen was the working electrode. The EIS was measured in the frequency range of 100 kHz to 0.01 Hz with an amplitude of 10 mV. The scanning speed was 2 mV/s and the anode scanning range was +500 mV in the potentiodynamic polarization test.

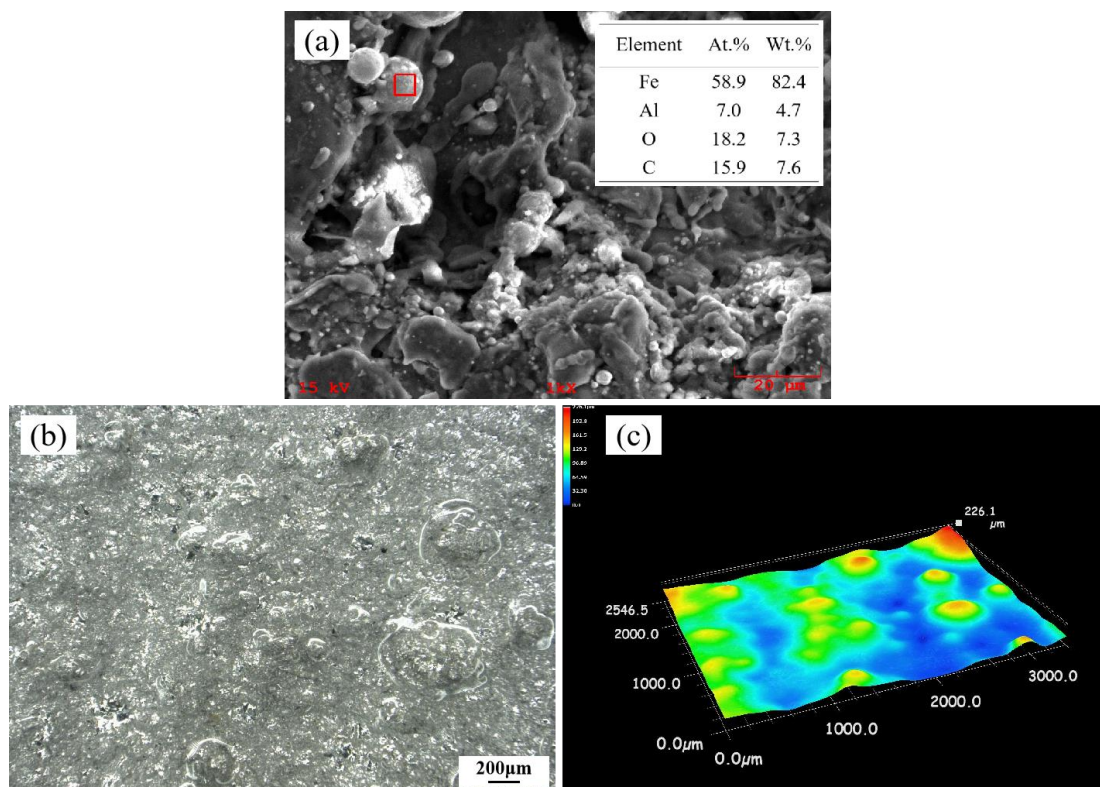
The specimens were removed after 32 days of soaking in different solutions and rinsed with distilled water to clean the residual sodium chloride on the surface and then blown dry with cold air. The morphology of the specimens before and after full immersion were observed by using 3D microscope (VHX-2000) and scanning electron microscope (SEM, su1510), and the elemental analysis of the specimen surface was performed by using the EDS spectrometer that comes with the scanning electron microscope.

The weight of the specimens before and after each set of experiments was measured to obtain the weight loss data of the specimens, and each set of data measurements was repeated three times, and finally the initial prediction of the coating service life was made.

### 3. RESULTS AND DISCUSSION

#### 3.1 Observation of the original morphology

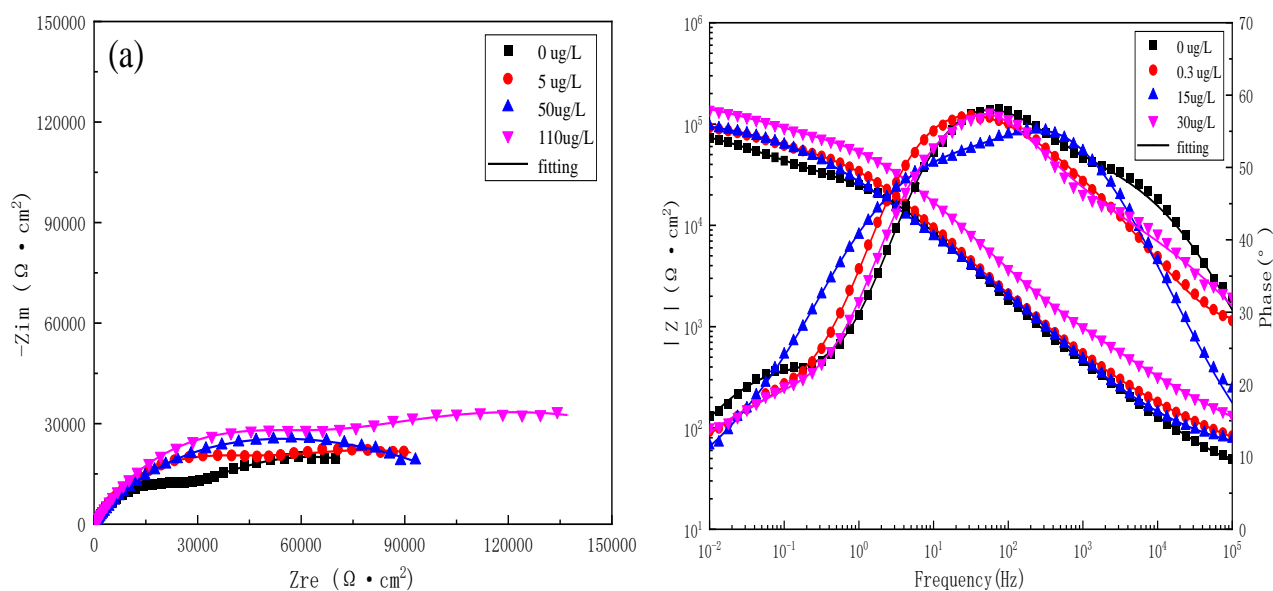
The original morphology of the coating and results of surface EDS analysis are presented in Fig. 1 (a). The surface of the specimen without a sealant applied demonstrates a typical molten stacking state with obvious holes and spherical objects. Analysis of the spherical object composition by EDS indicates that they are iron-carbon inclusions. These may be artefacts from preparation of the aluminum alloy. A large number of micro-couples will form around the inclusions on the coating surface when immersed in solution, potentially resulting in local corrosion and reducing corrosion resistance. Holes on the coating surface will become channels for diffusing solutions, causing corrosion inside the coating and adversely affecting the coating structure. From fig. 1 (b) and (c), it can be observed that after coating the specimen sealer, the surface of the coating is flatter with a height difference of only 226.1  $\mu\text{m}$ . This primarily comes from the coating itself, while the sealer can cover intercalated phases and pores on the surface of the coating, effectively preventing the solution from penetrating the surface [25]. However, weak spots will inevitably appear on the sealer surface, and corrosion may first occur in these areas.



**Figure 1.** (a) Surface morphology and local EDS analysis of the coating before sealing, (b) surface macroscopic morphology and (c) 3D topography after coating with sealant

### 3.2. Electrochemical test

The results obtained from electrochemical impedance spectroscopy (EIS) measurements of the specimens are shown in Fig. 2 (a)-(c), respectively. The Nyquist plots demonstrate that the specimens exhibit a capacitive arc during immersion. However, the radius of the capacitive arcs changes significantly with the prolonging of the immersion period. After 8 days the radius of capacitive arc gradually increased with an increase of copper concentration, indicating enhanced corrosion resistance. After 16 days of immersion, the radius of capacitive arc resistance showed a trend of increasing and then decreasing, while it gradually decreased after 32 days with the increase of copper ion concentration, indicating that the corrosion resistance of the specimen weakened. Analysis of the phase angle diagram in the Bode plots demonstrates three peaks appearing in the curve after 8 days of immersion, while there are only two peaks or a broad peak after 16 and 32 days of immersion. The electrochemical process of the specimen after 8 days of immersion is best fitted with the equivalent circuit  $R_s(Q_2R_2)(Q_1(R_1(Q_{dl}R_{ct})))$ , and is fitted with the equivalent circuit  $R_s(Q_{film}(R_{film}(Q_{dl}R_{ct})))$  after 16 and 32 days of immersion, where  $R_s$  represents the solution resistance,  $R_{film}$  and  $CPE_{film}$  represent the resistance and capacitance of the corrosion product film,  $R_{ct}$  represents the charge transfer resistance, and  $CPE_{dl}$  represents the electric double layer capacitance [31]. All capacitances in the circuit were replaced with constant phase angle elements (CPE) to compensate for the effects caused by the inhomogeneity of the specimen surface [32]. Compared to increased periods of immersion,  $R_2$  and  $CPE_2$  in the equivalent circuit of the specimen after 8 days represent the resistance and capacitance of a sparse porous film layer on the surface of the coating. The equivalent circuit and electrochemical impedance spectra show that there is a dynamic process of dissolution of the surface film layer and generation of a corrosion product film layer during immersion. The high frequency capacitive arc in the EIS plots represents the characteristics of the corrosion products formed on the coating surface, and the low-frequency capacitive arc is indicative of the electrochemical reflection characteristics.



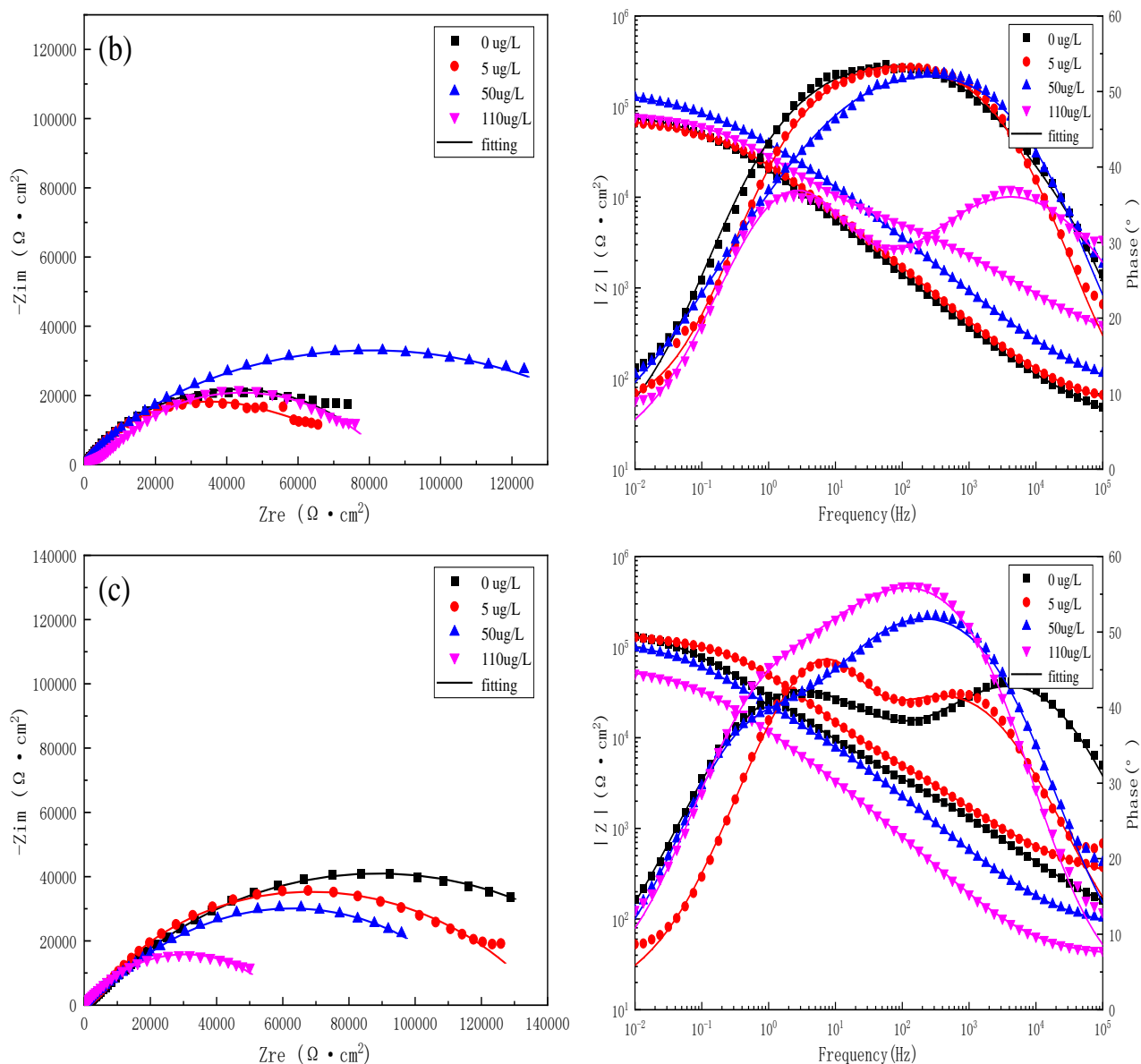


**Figure 2.** EIS of 5052 coated specimens immersed in 3.5% wt. NaCl solutions with  $Cu^{2+}$  concentrations of 0, 5, 50 and 110 ug/L for different days: (a) 8d, (b) 16d and (c) 32d

The data was fitted to obtain the polarization resistance ( $R_p$ ) of the specimens in each solution and these results are listed in Table 1. These demonstrate that  $R_p$  gradually increased after 8 days of immersion, indicating an increase in corrosion resistance in the short term. After 16 days this decreased, indicating that the high concentrations of copper ions accelerated the destruction of the surface film layer, with the  $R_p$  value gradually decreasing from  $1.34 \times 10^5 \Omega \cdot cm^2$  to  $5.16 \times 10^4 \Omega \cdot cm^2$  after 32 days of immersion, demonstrating a significant reduction in diffusion resistance. The above results show that low concentrations of copper promote the generation of a film of surface corrosion products, while high concentrations of copper ions significantly damage the passive film and accelerate the corrosion process.

**Table 1.** The  $R_p$  value of specimens with different days of immersion in solutions with different concentrations of  $\text{Cu}^{2+}$ 

Days	$R_p/(\Omega \cdot \text{cm}^2)$			
	0 $\mu\text{g} \cdot \text{L}^{-1}$	5 $\mu\text{g} \cdot \text{L}^{-1}$	50 $\mu\text{g} \cdot \text{L}^{-1}$	110 $\mu\text{g} \cdot \text{L}^{-1}$
8	7.36E+4	9.39E+4	9.48E+4	1.41E+5
16	7.44E+4	6.73E+4	1.27E+5	7.80E+4
32	1.34E+5	1.28E+5	9.96E+4	5.16E+4

The results of additional measurements of the potentiodynamic polarization curves are presented in Fig. 3. These demonstrate that the coatings exhibit slight passive behavior at the surface after a certain time of immersion in different solutions. The cathodic behavior is similar, with oxygen reduction and hydrogen precipitation reactions occurring, and the latter reactions dominating, as shown in equations (1) and (2) below:



As evident from equations (1) and (2), the copper ion concentration primarily affects the anodic reaction. As the solution penetrates the coating, the combined effect of the chloride ions and the precipitation of hydrogen from the coating surface causes local damage to the sealer, resulting in the exposure of the coating surface to the solution, whereupon the following reactions occur at the anode as shown in equations (3) and (4):



Solubilized  $\text{Al}^{3+}$  will diffuse into the solution, reacting with  $\text{OH}^-$  to generate  $\text{Al}(\text{OH})_3$  product that covers the surface of the coating, forming a protective film.

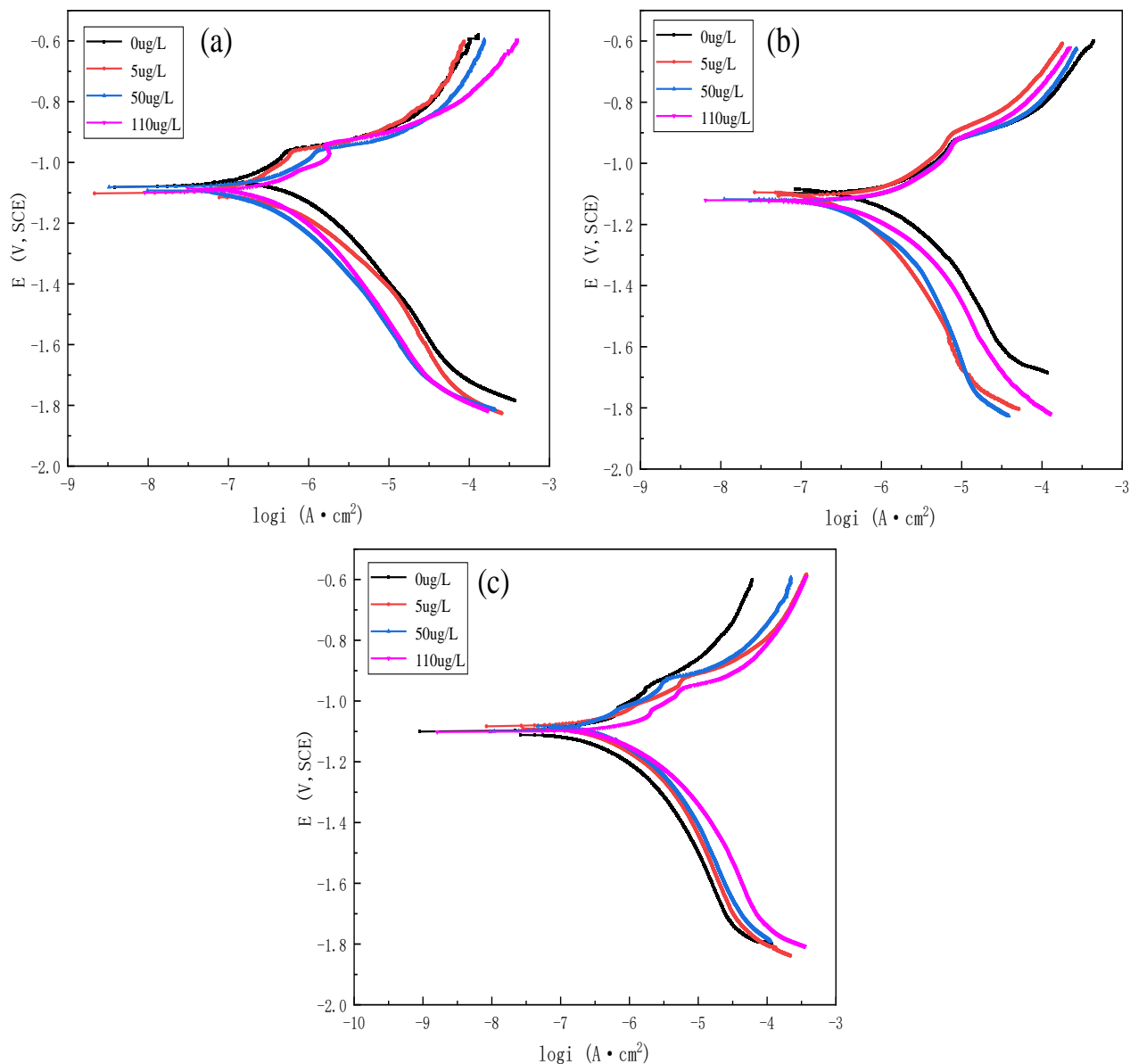


**Figure 3.** Polarization curves of specimens immersed in 3.5% wt. NaCl solutions with  $\text{Cu}^{2+}$  concentrations of 0, 5, 50 and 110  $\mu\text{g/L}$  for different days: (a) 8d, (b) 16d and (c) 32d

The corrosion characteristic parameters, such as the self-corrosion potential ( $E_{\text{corr}}$ ), self-corrosion current density ( $I_{\text{corr}}$ ) and anodic Tafel slope ( $B_a$ ) were obtained from the polarization curves and are presented in Table 2. The  $E_{\text{corr}}$  of the specimens in each solution does not differ significantly during the immersion process, and the  $I_{\text{corr}}$  is maintained in a low range, demonstrating that the corrosion rate of the coating is very small after the coating sealer is applied. After 8 days of immersion, any change in  $I_{\text{corr}}$  relative to the concentration of copper in solution is not evident, which is primarily due to the solution not penetrating the interior of the coating. After 16 days the solution penetrated into the interior of the coating causing coating surface weaknesses to occur at points of surface corrosion. At copper concentrations of and 5  $\mu\text{g/L}$ , the  $I_{\text{corr}}$  gradually increased with the concentration, explained by reaction (4), where copper ions resulted in the formation of galvanic couples between the copper monomers and

aluminum, where aluminum acting as the anode will be corroded. This has previously been reported by Wang [33] in an analogous situation. Subsequently, the generated corrosion products cover the defects and provide a measure of protection from the bulk solution. When the copper concentration reached 110 ug/L, the corrosion rate was significantly accelerated, resulting in an increase in  $I_{\text{corr}}$ ; after 32 days of immersion. It can be seen that the  $I_{\text{corr}}$  gradually increased with the concentration of copper, which is due to the fact that after a long period of immersion, the solution has penetrated into the coating through the defects on the surface. Precipitated hydrogen also promotes damage of the coating, with this behavior also reported by Chu [34] during studies of the corrosion of magnesium alloys. This result is consistent with the EIS results.

**Table 2.** Polarization parameters of specimens

Immersion time/d	Concentration/(ug·L <sup>-1</sup> )	$E_{\text{corr}}$ (vs.SCE)/mV	$I_{\text{corr}}$ /( $\mu\text{A}\cdot\text{cm}^{-2}$ )	$B_a$ /(mV·dec <sup>-1</sup> )
8	0	-1082	0.2014	279
	5	-1102	0.2443	329
	50	-1082	0.2912	366
	110	-1100	0.2135	374
16	0	-1097	1.112	158
	5	-1106	1.072	175
	50	-1123	0.9528	256
	110	-1121	1.768	143
32	0	-1100	0.3243	187
	5	-1083	0.7655	179
	50	-1099	1.317	123
	110	-1103	1.983	107

### 3.3 Surface morphology and weight loss analysis

The different severity of corrosion (Fig. 4) is directly related to the copper ion concentration of the solution and the condition of the coating surface. Under the same surface conditions, the number of corrosion pits on the surface increases significantly with the increase in copper ion concentration. In the control solution without copper present, the quantity of pits on the surface is lowest and the bottom of the pits is covered by an obvious white corrosion product. This corrosion product can form a protective layer separating the exposed pit surface from the solution. In the solution with a copper concentration of 5 ug/L the number of pits increased and yellow corrosion products were observed. The bottom of the corrosion pits was still covered by a small quantity of white corrosion products at this time. As the copper concentration was increased to 50 and 110 ug/L, the number of pits on the surface of the coating increased concurrently, as did the amount of yellow corrosion products observed. At these higher copper concentrations corrosion pits began to connect with each other. The corrosion products at the bottom of

the pits were observed to reduce similar to the phenomenon reported in the study conducted by Zhang [35]. This would cause the fresh coating at the bottom of pits to be exposed to the solution, reducing the resistance to ion diffusion resulting in a decrease of corrosion resistance, consistent with electrochemical test results

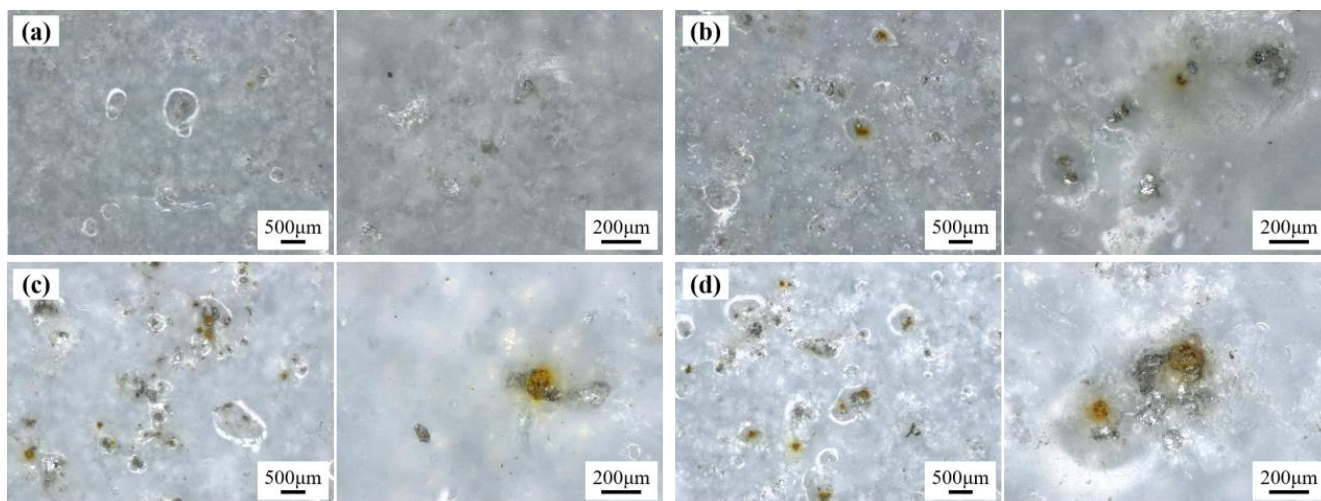


**Figure 4.** Surface morphology of the specimens after 32 days of immersion in 3.5% wt. NaCl solutions with  $\text{Cu}^{2+}$  concentrations of 0, 5, 50 and 110  $\mu\text{g/L}$ : (a) 0  $\mu\text{g/L}$ , (b) 5  $\mu\text{g/L}$ , (c) 50  $\mu\text{g/L}$  and (d) 110  $\mu\text{g/L}$

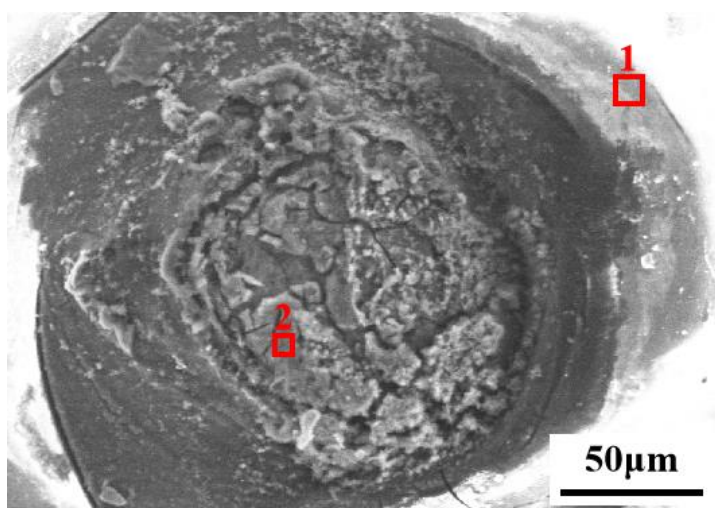


**Figure 5.** The local EDS analysis of the bottom of the pit on the coating surface after 32 days of immersion in a solution with 110  $\mu\text{g/L}$   $\text{Cu}^{2+}$

The results of EDS analysis of the bottom of the corrosion pits after 32 days of immersion with a copper ion concentration of 110  $\mu\text{g/L}$  are presented in Fig. 5 and Table 3. The bottom of the pits on the coating surface can be seen to be significantly stripped of the sealer and the C content is significantly reduced relative to fresh surfaces. The Al content is increased indicating that the coating surface has

been exposed to the solution and cracks can be seen on the surface as well as a small amount of spalling. The content of Cu at the bottom of the pits is increased, demonstrating that copper ions are deposited on the aluminum surface and accelerate the corrosion of the coating.

**Table 3.** The results of local EDS analysis of the coating surface

Element	Region 1		Region 2	
	At.%	Wt.%	At.%	Wt.%
C	60.8	52.7	10.3	6.6
O	37.4	43.2	65.4	55.6
Al	1.3	2.5	22.0	31.5
Cu	0.1	0.5	1.3	4.4
Cl	0.4	1.1	1.0	1.9

The weight loss of the specimens was measured after 32 days of immersion in the 3.5% wt. NaCl solutions with the results presented in Fig. 6. When the concentration of copper ions was low, the weight loss of the coating was effectively unchanged, while the weight loss of the specimens increased significantly with copper content. After 32 days of immersion in NaCl solution containing 110  $\mu\text{g/L}$  copper(II), the weight loss of the specimens was 5.4 mg, a similar trend as the changes of the surface morphology of the coating.

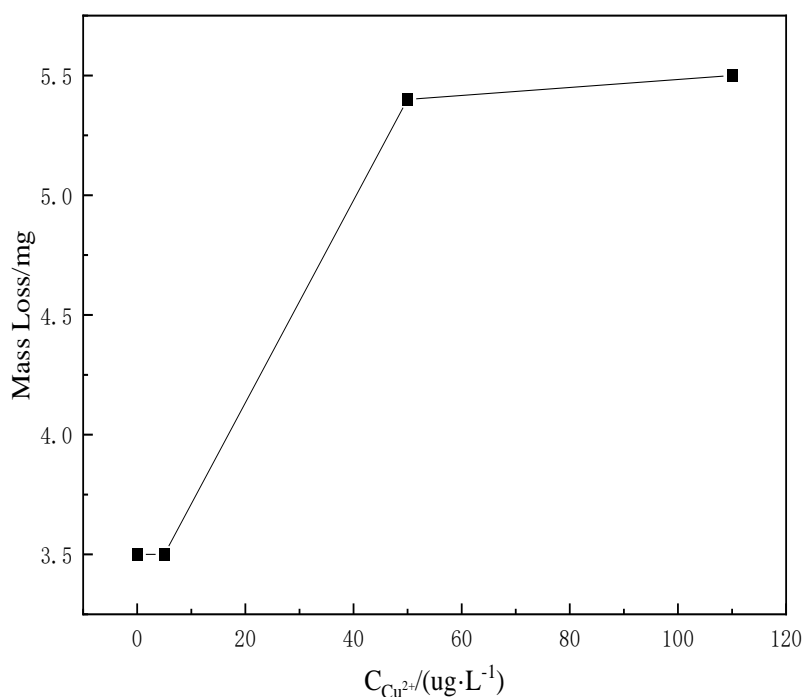


**Figure 6.** Weight loss data of specimens after 32 days of immersion in 3.5% wt. NaCl solutions with  $\text{Cu}^{2+}$  concentrations of 0, 5, 50 and 110  $\mu\text{g/L}$

#### 4. CONCLUSION

1) The concentration of copper ions in the 3.5% wt. NaCl solution demonstrated favorable effects on the corrosion resistance of the composite coatings commonly used in ORV for a short period of time. Unfavorable effects were evident under periods of prolonged immersion (up to 32 days), and the corrosion resistance of the specimens gradually decreased with the increase of copper ion concentration.

2) The destructive effect of seawater containing copper ions on the coating comes from the destruction of the oxide film by  $\text{Cl}^-$  ions and the displacement deposition of  $\text{Cu}^{2+}$  ions to form a galvanic couple that accelerates the corrosion of aluminum. Coating surface integrity has a direct impact on the corrosion resistance, and localized corrosion occurs preferentially at the site of defects on the sealant surface.

3) The capacitive properties appear under full immersion conditions, probably due to the corrosion process occurring on the coating surface film. The weight loss increased from 4.5 mg to 5.4 mg after a 32 days immersion as the concentration of copper increased.

#### ACKNOWLEDGEMENTS

This work was supported by Research on ORV Corrosion Mechanism and Application of Prevention and Control Technology (2019-XSKJ-04), Tianjin Science and Technology Project (No.20YDTPJC01780), and Shandong Taishan Industry Leading Talents Project (No.SF1503302301).

#### References

1. B. Wang, X.H. Chen, F.S. Pan, J.J. Mao and Y. Fang, *Trans. Nonferrous Met. Soc. China*, 25 (8) (2015) 2481.
2. W.J. Qi, X. Qi, B. Sun, C. Wang, J.R. Jin and R.G. Song, *Mater. Performance*, 56 (11) (2017) 58.
3. C.Y. Meng, D. Zhang, C. Hua, L.Z. Zhang and J.S. Zhang, *J. Alloys Compd.*, 617 (25) (2014) 925.
4. W.S. Miller, L. Zhuang, J. Bottema, A.J. Wittebrood, P.De. Smet, A. Haszler and A. Vieregge, *Mater. Sci. Eng., A*, 280 (1) (2000) 37.
5. C.M. Liao and R.P. Wei, *Electrochim. Acta*, 45 (6) (1999) 881.
6. Z. Szklarska-Smialowska, *Corros. Sci.*, 41 (9) (1999) 1743.
7. F. Deflorian, S. Rossi and S. Prosseda, *Mater. Des.*, 27 (9) (2006) 758.
8. G.S. Frankel, *J. Electrochem. Soc.*, 145 (6) (1998) 2186.
9. N. Sridhar, C.S. Brossia, D.S. Dunn and A. Anderko, *Corrosion*, 60 (2004) 915.
10. V.S. Sinyavskii and V.D. Kalinin, *Prot. Met.*, 41 (4) (2005) 317.
11. R.G. Buchheit, R.P. Grant, P.F. Hlava, B. Mckenzie and G.L. Zender, *J. Electrochem. Soc.*, 144(8) (1997) 2621.
12. M. Tadjamoli, M. Tzinmann and C. Fiaud, *Br. Corros. J.*, 19 (1) (1984) 36.
13. Y. Zhao, Z.G. Qi, Q.R. Wang, J.P. Chen and J. Shen, *Exp. Therm Fluid Sci.*, 37 (2012) 98.
14. M.S. Hong, I.J. Park and J.G. Kim, *Met. Mater. Int.*, 23 (4) (2017) 708.
15. V. Uksien, K. Leinartas, R. Jušknas, A. Sudavičius and E. Juzeliūnas, *Electrochem. Commun.*, 4 (10) (2002) 747.
16. M.G.A. Khedr and A.M.S. Lashien, *J. Electrochem. Soc.*, 136 (4) (1989) 968.
17. X. Joseph Raj and N. Rajendran, *J. Fail. Anal. Prev.*, 19 (2019) 250.
18. S.L. Gao, M. Yu, J.H. Liu, B. Xue and S.M. Li, *Int. J. Miner. Metall. Mater.*, 24 (4) (2017) 423.
19. H. Hu, N. Li, J.N. Cheng and L.J. Chen, *J. Alloys Compd.*, 472 (1-2) (2009) 219.

20. Y. Bai, Z.H. Wang, X.B. Li, G.S. Huang, C.X. Li and Y. Li, *J. Alloys Compd.*, 7189 (30) (2017) 194.
21. H.R. Bakhsheshi-Rad, E. Hamzah, H.T. Low, M. Kasiri-Asgarani, S. Farahany, E. Akbari and M.H. Cho, *Mater. Sci. Eng., C*, 73 (1) (2017) 215.
22. M. Mozetič, *Mater.*, 12 (3) (2019) 441.
23. C.V. Moraes, R.J. Santucci Jr., J.R. Scully and R.G. Kelly, *J. Electrochem. Soc.*, 168 (5) (2021) 168.
24. X.W. Zeng, Y. Liu and Z.L. Bai, *Coatings*, 9(12) (2019) 867.
25. L. Hao and B. Rachel Cheng, *Met. Finish.*, 98 (12) (2000) 8.
26. X.W. Li, T. Shi, B. Li, X.C. Chen, C.W. Zhang, Z.G. Guo and Q.X. Zhang, *Mater. Des.*, 183 (5) (2019) 108152.
27. G. Yoganandan, J.N. Balaraju, C.H.C. Low, G.J. Qi and Z. Chen, *Surf. Coat. Technol.*, 288 (25) (2016) 115.
28. A.A. Seman, J.K. Chan, M.A. Norazman, Z. Hussain, D. Brij and A. Ismail, *Anti-Corros. Methods Mater.*, 67 (1) (2020) 7.
29. S. Shamsudeen and E.R.D. John, *Mater. Perform. Charact.*, 8 (4) (2019) 555.
30. C.K. Chung, C.H. Tsai, C.R. Hsu, E.H.Kuo, Y. Chen and I.C. Chung, *Corros. Sci.*, 125 (15) (2017) 40.
31. H.X. Chen and D.J. Kong, *Mater. Chem. Phys.*, 251 (1) (2020) 123200.
32. J.D. Zuo, B. Wu, C.Y. Luo and F. Xing, *Corros. Sci.*, 152 (15) (2019) 120.
33. X.H. Wang, Z.W. Peng, L. Ma, Y.H. Lin, G.X. Li and H.L. Wang, *Int. J. Electrochem. Sci.*, 12 (2017) 11006.
34. P.W. Chu, E.L. Mire and E.A. Marquis, *Corros. Sci.*, 128 (2017) 253.
35. K. Zhang, B.W. Wen, L.W. Zhang, C. Li, J. Liu and P. Yi, *Int. J. Electrochem. Sci.*, 15 (2020) 11036.

© 2021 The Authors. Published by ESG ([www.electrochemsci.org](http://www.electrochemsci.org)). This article is an open access article distributed under the terms and conditions of the Creative Commons Attribution license (<http://creativecommons.org/licenses/by/4.0/>).